Atmospheric chemistry of HCFC-133a: The UV absorption spectra of CF3CClH and CF3CClHO2 radicals, reactions of CF3CClHO2 with NO and NO2, and fate of CF3CClHO radicals

4 **AUTHORS**, INCLUDING:

Ole John Nielsen
University of Copenhagen

263 PUBLICATIONS **5,000** CITATIONS

Atmospheric Chemistry of HCFC-133a: The UV Absorption Spectra of CF_3CClH and CF_3CClHO_2 Radicals, Reactions of CF_3CClHO_2 with NO and NO_2, and Fate of CF_3CClHO Radicals

Trine E. Møgelberg, Ole J. Nielsen,* and Jens Sehested

Section for Chemical Reactivity, Environmental Science and Technology Department,
Risø National Laboratory, DK-4000 Roskilde, Denmark

Timothy J. Wallington*

Ford Research Laboratory, SRL-3083, Ford Motor Company, Dearborn, P.O. Box 2053, Michigan 48121-2053
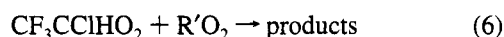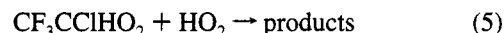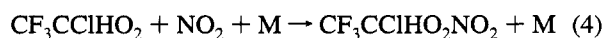
Received: December 19, 1994; In Final Form: June 23, 1995[®]

The UV absorption spectra of CF_3CClH and CF_3CClHO_2 radicals have been investigated. The CF_3CClH spectrum was quantified over the wavelength range 225−280 nm. The absorption cross section at 250 nm was $(139 \pm 16) \times 10^{-20}$ cm^2 molecule^{-1}. The absorption spectrum for CF_3CClHO_2 was quantified over the wavelength range 225−290 nm, and at 250 nm $\sigma_{250 \text{ nm}} = (258 \pm 30) \times 10^{-20}$ cm^2 molecule^{-1}. The kinetics of the reactions of the peroxy radical CF_3CClHO_2 with NO and NO_2 were studied and the derived rate constants were $k_3 = (1.0 \pm 0.3) \times 10^{-11}$ cm^3 molecule^{-1} s^{-1} and $k_4 = (6.4 \pm 1.5) \times 10^{-12}$ cm^3 molecule^{-1} s^{-1}, respectively. The self-reaction rate for the CF_3CClHO_2 radicals was measured and a value of $k_{6obs} = (4.4 \pm 0.3) \times 10^{-12}$ cm^3 molecule^{-1} s^{-1} was obtained. The reactions of F atoms with CF_3CH_2Cl and of CF_3CClH with O_2 were found to proceed with rate constants of $k_8 = (2.0 \pm 0.6) \times 10^{-12}$ cm^3 molecule^{-1} s^{-1} and $k_2 = (1.4 \pm 0.1) \times 10^{-12}$ cm^3 molecule^{-1} s^{-1}, respectively. The reaction of CF_3CClHO_2 radicals with NO gives NO_2, and by implication CF_3CClHO radicals, which in the atmosphere (a) react with O_2 to give $CF_3C(O)Cl$ and (b) decompose to give, most likely, CF_3 radicals and $HC(O)Cl$. In 700 Torr of N_2 diluent the rate constant ratio $k_{O_2}/k_{diss} = (2.1 \pm 0.4) \times 10^{-19}$ cm^3 molecule^{-1}. As part of the present work, relative rate techniques were used to measure rate constants for the reactions of Cl and F atoms with CF_3CH_2Cl of $(6.8 \pm 1.2) \times 10^{-15}$ and $(2.1 \pm 0.5) \times 10^{-12}$ cm^3 molecule^{-1} s^{-1}, respectively. All experiments were performed at 296 ± 2 K.

1. Introduction

As agreed in the latest amendment to the Montreal Protocol, the production of CFCs is to be phased out by the end of 1995. Hydrofluorocarbons (HFCs) and hydrochlorofluorocarbons (HCFCs) are important CFC replacements. To place discussions of the environmental impact of HFCs and HCFCs on a sound technical basis requires a detailed knowledge of their atmospheric chemistry. As part of a collaboration between our laboratories to survey the atmospheric chemistry of important HFCs and HCFCs, we have investigated HCFC-133a, CF_3CH_2Cl. This compound is not of present commercial importance, although it is structurally similar to HFC-134a (CF_3CH_2F) which is of a major economic importance. Information on the chemistry of HCFC-133a may provide an interesting comparison with the atmospheric chemistry of HFC-134a.

In contrast to CFCs, HCFCs and HFCs have C−H bonds and are susceptible to attack by OH radicals in the lower atmosphere. Reactions that are expected to be important in the atmospheric chemistry of HCFC-133a are as follows:[1]

$$CF_3CH_2Cl + OH \rightarrow CF_3CClH + H_2O \quad (1)$$

$$CF_3CClH + O_2 + M \rightarrow CF_3CClHO_2 + M \quad (2)$$

$$CF_3CClHO_2 + NO \rightarrow CF_3CClHO + NO_2 \quad (3)$$

$$CF_3CClHO_2 + NO_2 + M \rightarrow CF_3CClHO_2NO_2 + M \quad (4)$$

$$CF_3CClHO_2 + HO_2 \rightarrow products \quad (5)$$
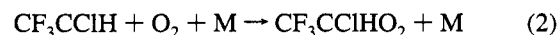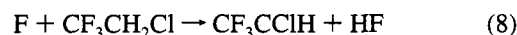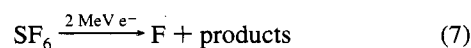
$$CF_3CClHO_2 + R'O_2 \rightarrow products \quad (6)$$

In the present work, we have studied the kinetics of reactions 2−4 and 6 using a pulse radiolysis technique. In addition, the fate of the alkoxy radical CF_3CClHO was determined using a FTIR−smog chamber system. Results are reported herein.

2. Experimental Section

Two different experimental systems were used in the present work. Both experimental systems have been described in detail in previous publications[2,3] and will only be discussed briefly here.

2.1. Pulse Radiolysis System. $CF_3CH_2Cl/O_2/SF_6$ mixtures were radiolyzed in a 1 L stainless steel reaction cell using a 30 ns pulse of 2 MeV electrons from a Febetron 705B field emission accelerator. SF_6 was always in great excess and was used to generate fluorine atoms:

$$SF_6 \xrightarrow{\text{2 MeV e}^-} F + products \quad (7)$$

$$F + CF_3CH_2Cl \rightarrow CF_3CClH + HF \quad (8)$$

$$CF_3CClH + O_2 + M \rightarrow CF_3CClHO_2 + M \quad (2)$$

UV absorptions attributed to transient radical species were followed by multipassing the output of a pulsed 150 W xenon arc lamp through the reaction cell using internal White cell optics. Total path lengths of 80 and 120 cm were used. After

**13438** *J. Phys. Chem., Vol. 99, No. 36, 1995*

Møgelberg et al.

passing through the cell the light was guided through a 1 m McPherson grating UV—vis monochromator and detected with a Hamamatsu photomultiplier. The spectral resolution was 0.8 nm. Reagent concentrations used were SF_6, 900—950 mbar; O_2, 0—40 mbar; CF_3CH_2Cl, 0—50 mbar; NO, 0.23—0.88 mbar; and NO_2, 0.24—0.81 mbar. All experiments were performed at 296K. Ultra high purity O_2 was supplied by L'Air Liquide, SF_6 (99.9%) was supplied by Gerling and Holz, NO(99.8%) from Messer Grieshem, and CF_3CH_2Cl (>97%) was obtained from Fluorochem. All reagents were used as received. FTIR spectroscopy was used to search for impurities in the CF_3CH_2-Cl sample; none were found. The partial pressures of the different gases were measured using a Baratron membrane manometer with a resolution down to 10^{-5} bar.

Seven sets of experiments were performed using the pulse radiolysis system. First, the spectrum of CF_3CClH was recorded by observing the maximum transient absorption following pulse radiolysis of mixtures of 30 mbar CF_3CH_2Cl and 970 mbar of SF_6. Second, the rate constant for the reaction of F atoms with CF_3CH_2Cl was determined by monitoring the maximum transient absorption following the radiolysis of $CF_3CH_2Cl/O_2/SF_6$ mixtures as a function of the $[CF_3CH_2Cl]/[O_2]$ ratio. Third, the UV spectrum of CF_3CClHO_2 was recorded by observing the maximum transient absorption following the radiolysis of $CF_3CH_2Cl/O_2/SF_6$ mixtures. Fourth, the rate constant for the reaction between CF_3CClH with O_2 was measured by varying the O_2 concentration and studying the rate of formation of the CF_3CClHO_2 radical at short times (20 μs). Fifth, the rate constant for the self-reaction of CF_3CClHO_2 radicals was determined by studying the dependence of the rate of decay of the transient absorption on the initial radical concentration using $CF_3CH_2Cl/O_2/SF_6$ mixtures. Sixth, the rate of reaction 3 was determined by adding NO to the mixture and monitoring the rate of formation of NO_2 at 400 nm. Seventh, the rate of reaction of CF_3CClHO_2 radicals with NO_2 was determined using the radiolysis of $CF_3CH_2Cl/O_2/SF_6/NO_2$ mixtures with the NO_2 loss rate monitored at 400 nm.

2.2. FTIR—Smog Chamber System. The FTIR system was interfaced to a 140 L Pyrex reactor. Radicals were generated by the UV irradiation of mixtures of 69—1100 mTorr of CF_3-CH_2Cl, 0.2—0.4 Torr of Cl_2 or 0.2—0.5 Torr of F_2, and 2.3—700 Torr of O_2 in 700 Torr total pressure with N_2 diluent at 296 K using 22 blacklamps (760 Torr = 1013 mbar). The loss of reactants and the formation of products were monitored by FTIR spectroscopy, using an analyzing path length of 27 m and a resolution of 0.25 cm^{-1}. Infrared spectra were derived from 32 co-added spectra. CF_3CH_2Cl, $CF_3C(O)Cl$, CF_3CHO, and $HC(O)Cl$ were monitored using their characteristic features over the wavenumber ranges 770—870, 720—900 and 1750—1850, 700—750 and 1750—1850, and 710—760 cm^{-1}, respectively. Reference spectra were acquired by expanding known volumes of reference materials into the reactor.

3. Results

3.1. Pulse Radiolysis System. *UV Absorption Spectrum of CF_3CClH Radicals.* The UV absorption spectrum was studied by observing the maximum transient absorption at short times (40 μs) following the radiolysis of mixtures of 30 mbar of CF_3-CH_2Cl and 970 mbar SF_6. The spectrum was quantified in the wavelength range 225—275 nm. The UV path length was 80 cm. An example of an absorption transient is given in Figure 1. A series of experiments at 250 nm using different radiolysis doses was performed to determine conditions where F atoms are converted stoichiometrically into CF_3CClH radicals. In Figure 2, the maximum absorption is plotted as a function of radiolysis dose. The datapoint at zero radiolysis dose was
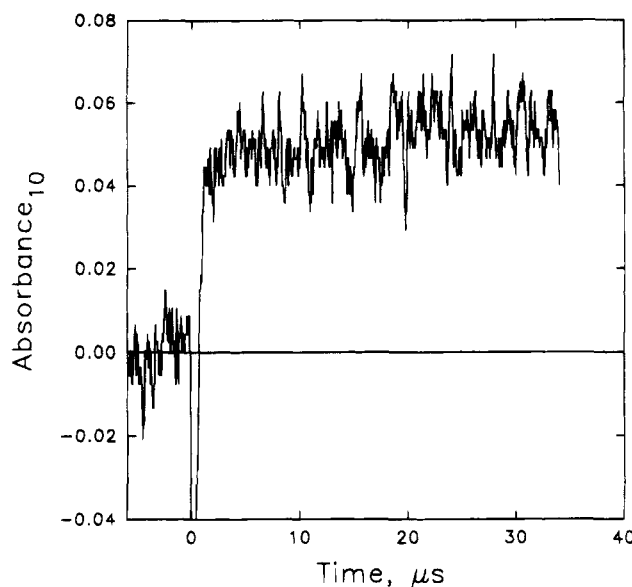
Figure 1. Absorption transient for mixtures of 30 mbar of CF_3CH_2Cl and 970 mbar of SF_6 at 230 nm. The radiolysis dose used was 42% of full dose.
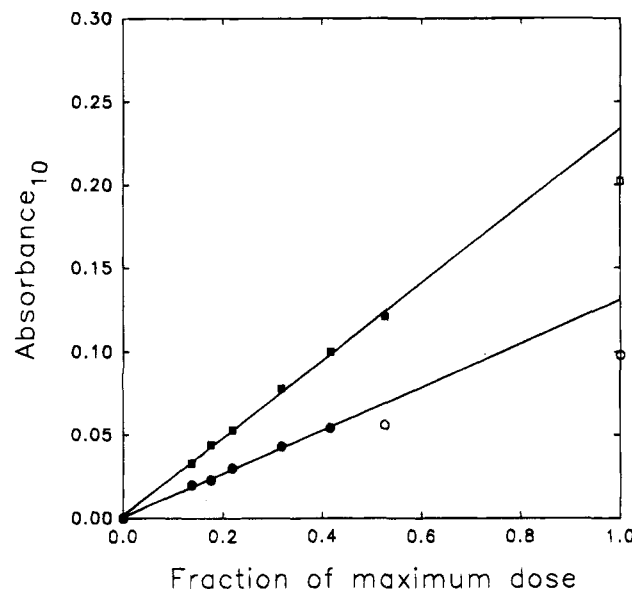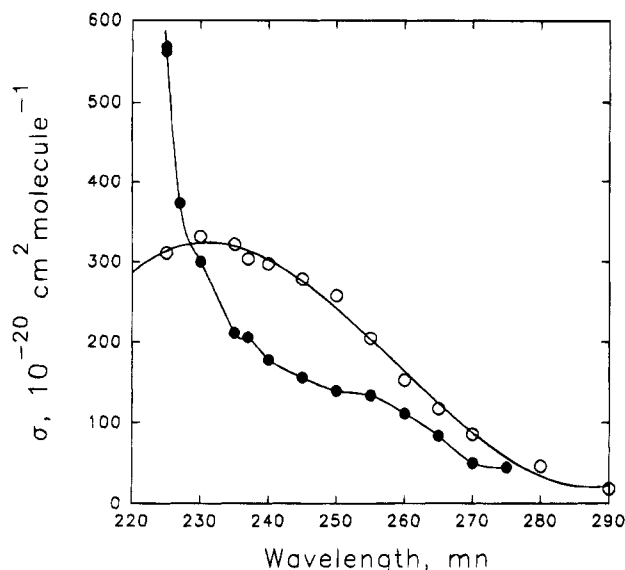
Figure 2. Maximum transient absorption (circles) as a function of radiolysis dose at 250 nm for mixtures of 30 mbar of CF_3CH_2Cl and 970 mbar of SF_6. The straight line is a linear least-squares fit through the low dose data. Maximum transient absorption (squares) vs radiolysis dose at 250 nm and 40 mbar of CF_3CH_2Cl, 20 mbar of O_2, and 940 mbar of SF_6.

obtained by filling the reaction cell with reactants, placing a stainless steel plate in between the electron source and cell and then firing the source. No transient absorption signal was observed, and hence the point at the origin in Figure 2. It can be seen that for doses less than 40% of full dose the maximum absorption is proportional to the radiolysis dose, and hence the initial F atom concentration. At higher doses the measured absorption is smaller than expected from a linear extrapolation of the low dose data. We ascribe this nonlinearity at high doses to unwanted radical—radical reactions such as

$$CF_3CClH + CF_3CClH \rightarrow products \qquad (9)$$

$$F + CF_3CClH \rightarrow products \qquad (10)$$
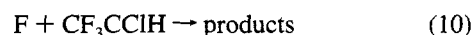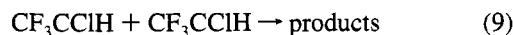
Using three pieces of information, (i) the F atom yield at full dose and 1000 mbar of SF_6, $(2.8 \pm 0.3) \times 10^{15}$ cm^{-3},[4] (ii) the slope (0.130 ± 0.004) of the linear least-squares fit through

Atmospheric Chemistry of HCFC-133a

J. Phys. Chem., Vol. 99, No. 36, 1995 **13439**

Figure 3. Absorption spectra for CF_3CClH radicals (closed symbols) and CF_3CClHO_2 radicals (open symbols).

TABLE 1: Measured Absorption Cross Sections for CF_3CClH and CF_3CClHO_2 Radicals

wavelength (nm)	$\sigma_{CF_3CClH} \times 10^{20}$ (cm² molecule⁻¹)	$\sigma_{CF_3CClHO_2} \times 10^{20}$ (cm² molecule⁻¹)
225	565	311
227	373	
230	301	331
235	212	322
240	178	297
245	156	279
250	139	258
255	134	205
260	111	153
265	84	117
270	50	85
275	45	
280		46
290		18

the low dose data in Figure 2, and (iii) the UV path length of 80 cm, we can calculate the absorption cross section of CF_3-$CClH$ at 250 nm to be $(139 \pm 16) \times 10^{-20}$ cm² molecule⁻¹. Quoted errors were derived using conventional error propagation analysis and reflect uncertainties associated with both the F atom yield and the measurement of the slope in Figure 2. To map out the spectrum, experiments were performed to measure the initial absorbance between 225 and 275 nm following the radiolysis pulse. The initial absorbances were scaled to that at 250 nm. The results are plotted in Figure 3 and given in Table 1.

The $F + CF_3CH_2Cl$ Reaction. To determine the rate constant for the $F + CF_3CH_2Cl$ reaction, O_2 was added to the system. After the radiolysis pulse, reactions 8 and 11 compete for the variable F atoms.

$$F + CF_3CH_2Cl \rightarrow CF_3CClH \tag{8}$$

$$F + O_2 + M \rightarrow FO_2 + M \tag{11}$$
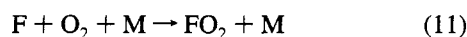
CF_3CClH radicals formed in reaction 8 will add O_2 to give the corresponding peroxy radicals.

$$CF_3CClH + O_2 + M \rightarrow CF_3CClHO_2 + M \tag{2}$$

A series of experiments was performed using a monitoring wavelength of 250 nm, reaction mixtures of 40 mbar of O_2, 950 mbar of SF_6, and 0–20.2 mbar of CF_3CH_2Cl, with the radiolysis dose fixed at 50% of full dose. Figure 4 shows the maximum transient absorption as a function of the [CF_3CH_2-
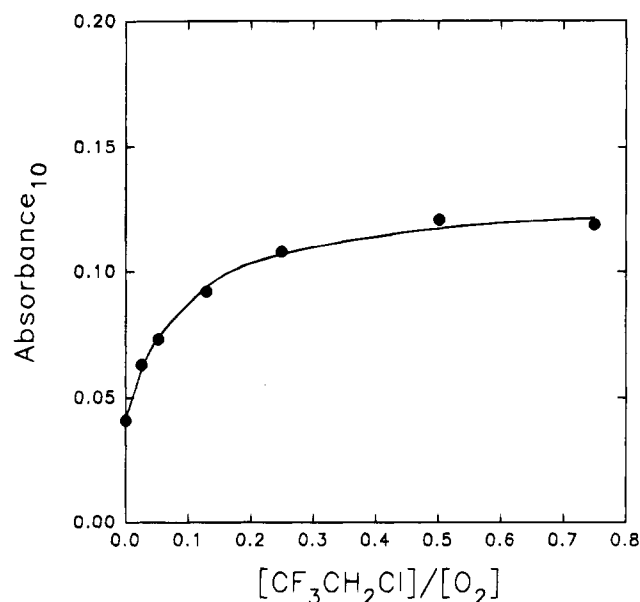
Figure 4. Maximum transient absorbance as a function of the [CF_3-CH_2Cl]/[O_2] ratio at 250 nm.

Cl]/[O_2] ratio. As seen from the figure, the absorption was small at low [CF_3CH_2Cl]/[O_2] ratios and increased as the [CF_3CH_2-Cl]/[O_2] ratio was increased to 0.5. Further increase in the [CF_3-CH_2Cl]/[O_2] ratio had no significant effect on the transient absorption maximum. At low CF_3CH_2Cl concentrations, FO_2 radicals are mainly formed and, on a per molecule basis, FO_2 radicals absorb less than CF_3CClHO_2 radicals. As the CF_3CH_2-Cl concentration is increased CF_3CClHO_2 radicals are formed at the expense of FO_2 radicals and the transient absorption maximum increases. The following expression was fit to the data:

$$A_{max} = \{A_{FO_2} + A_{CF_3CClHO_2}(k_8/k_{11})[CF_3CH_2Cl]/[O_2]\}/$$
$$\{1 + (k_8/k_{11})[CF_3CH_2Cl]/[O_2]\}$$

where A_{max} is the maximum absorbance, A_{FO_2} is the maximum absorbance expected if only FO_2 radicals are produced, and $A_{CF_3CClHO_2}$ is the maximum absorbance expected if CF_3CClHO_2 were the sole absorbing species. Parameters A_{FO_2}, $A_{CF_3CClHO_2}$, and k_8/k_{11} were varied simultaneously. The best fit was obtained with $k_8/k_{11} = (10.8 \pm 3.3)$. Quoted errors are 2 standard deviations. Using $k_{11} = 1.9 \times 10^{-13}$ cm³ molecule⁻¹ s⁻¹,[5] we derive $k_8 = (2.0 \pm 0.6) \times 10^{-12}$ cm³ molecule⁻¹ s⁻¹.

It is surprising that in Figure 4 the ratio of the asymptote to the y-axis intercept, $A_{CF_3CClHO_2}/A_{FO_2}$, is 2.75 compared to the expected value of 2.0 (2.58×10^{-18} [this work]/1.30×10^{-18} [ref 5]). The uncertainties in absorption cross sections for CF_3-$CClHO_2$ and FO_2 are both approximately 10%. Thus, we would expect the ratio to be within 10–20% of 2.0. The fact that it is not is probably due to uncertainties in measurement of the rather small absorbance in the absence of added CF_3CClH_2.

UV Absorption Spectrum of CF_3CClHO_2 Radicals. A series of experiments was performed to determine the optimal experimental conditions for converting F atoms into CF_3CClHO_2 radicals. Possible interfering secondary chemistry when radiolysing $CF_3CH_2Cl/O_2/SF_6$ mixtures include

$$CF_3CClHO_2 + CF_3CClH \rightarrow products \tag{12}$$

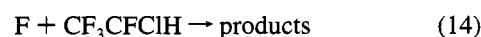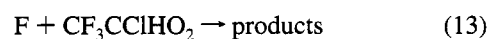$$F + CF_3CClHO_2 \rightarrow products \tag{13}$$

$$F + CF_3CFClH \rightarrow products \tag{14}$$

Figure 2 shows the maximum absorption vs the radiolysis dose for mixtures of 40 mbar of CF_3CClH_2, 20 mbar of O_2, and 940
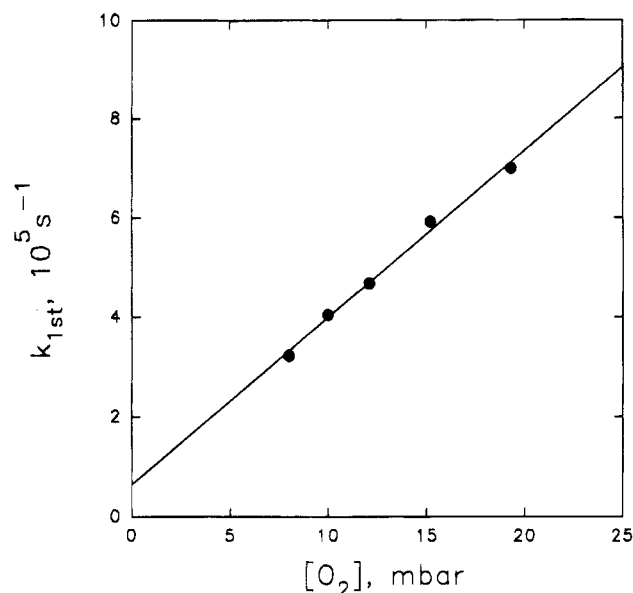
mbar of SF_6 at 250 nm. As seen from Figure 2, the maximum transient absorption increased linearly with the dose up to 50% of full dose. At full dose the maximum transient absorbance falls below that expected from a linear extrapolation of the low dose results. We ascribe this behavior to unwanted radical—radical reactions such as (12)—(14) at high initial radical concentration. A linear least-squares fit through the low dose data gives a slope of 0.23 ± 0.01.

The maximum transient absorbance following radiolysis of mixtures of 40 mbar of CF_3CH_2Cl, 20 mbar of O_2, and 940 mbar of SF_6 was studied at short times (40 μs). The radiolysis dose used was 50% of full dose and the absorption wavelength was varied between 225 and 290 nm. Due to the competition for F atoms via reactions 8 and 11 some of the F atoms will react with O_2 instead of CF_3CH_2Cl. With the pressures used and the rate constants $k_8 = (2.0 \pm 0.6) \times 10^{-12}$ cm^3 molecule^{-1} s^{-1} and $k_{11} = 1.9 \times 10^{-13}$ cm^3 molecule^{-1} s^{-1} we can calculate that 4.5% of the F atoms react with O_2. We therefore have to correct the measured absorbances for absorption by FO_2 radicals. Using the following information (i) the F atom yield of (2.8 ± 0.3) × 10^{15} [4] at full dose and 1000 mbar of SF_6, (ii) σ_{FO_2} (250 nm) = 130 × 10^{-20} cm^2 molecule^{-1},[5] and (iii) the slope of the straight line through the low dose data (0.23 ± 0.01), we calculate the absorption cross section for CF_3CClHO_2 at 250 nm to be (258 ± 30) × 10^{-20} cm^2 molecule^{-1}. The quoted errors reflect uncertainties in the slope of the data in Figure 2 and in the calculation of the F atom yield. To map out the spectrum, experiments were performed to measure the initial absorbance between 225 nm and 290 nm. The maximum initial absorbancies were scaled to that at 250 nm and corrected for FO_2 to obtain absolute absorption cross sections. The absorption cross sections are plotted in Figure 3 and listed in Table 1.
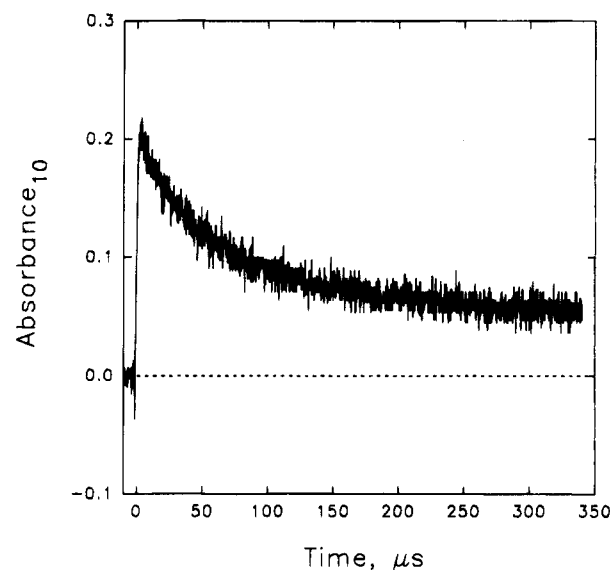
The CF_3CClH + O_2 Reaction. The reaction of CF_3CClH radicals with O_2 was studied by observing the formation of CF_3-$CClHO_2$ radicals following the radiolysis of $CF_3CClH_2/O_2/SF_6$ mixtures at short times (20 μs). The conditions were 50 mbar of CF_3CClH_2, 5.2—19.3 mbar of O_2, and SF_6 added up to 1 bar total pressure. The absorption transients were well fitted using first-order kinetics, pseudo-first-order rate constants are plotted as a function of the O_2 concentration in Figure 5. Linear least-squares analysis of the data in Figure 5 gives $k_2 = (1.4 \pm 0.1) \times 10^{-12}$ cm^3 molecule^{-1} s^{-1}.

The CF_3CClHO_2 Self-Reaction. Experiments were performed using 40 mbar of CF_3CH_2Cl, 20 mbar of O_2, and 940 mbar of SF_6 at a monitoring wavelength of 250 nm. The UV light path length was 80 cm and the radiolysis dose was varied. Figure 6 shows a typical transient absorption, following the pulse radiolysis of $CF_3CClH_2/O_2/SF_6$ mixtures. This decay can be fitted with a nonlinear least-squares second-order fit. We ascribe the decay to the CF_3CClHO_2 self-reaction. Figure 7 shows a plot of the reciprocal half-life obtained from the fit as a function of the initial maximum absorption. The straight line through the data is a linear least fit with a slope of (9.82 ± 0.37) × 10^4 s^{-1}. This slope is related to the rate constant for the self-reaction k_{6obs}, by the expression slope = (k_{6obs} × 2 ln(10))/(σ(CF_3-$CClHO_2$) × 80). Hence, we derive $k_{6obs} = (4.4 \pm 0.5) \times 10^{-12}$ cm^3 molecule^{-1} s^{-1}. Quoted errors reflect uncertainties in both σ(CF_3CClHO_2) and the slope in Figure 7.

The CF_3CClHO_2 + NO Reaction. To study the kinetics of reaction 3, experiments were performed where the transient absorption at 400 nm was monitored following radiolysis of $NO/CF_3CH_2Cl/O_2/SF_6$ mixtures. An example of an absorption trace is shown in Figure 8. The observed absorption is ascribed to the formation of NO_2 via reaction 3. To extract a value for k_3 from traces such as that shown in Figure 8 the trace was fitted by using the expression $A(t) = (A_\infty - A_0) \times [1 - \exp$-

Figure 5. Plot of the pseudo-first-order rate of CF_3CClHO_2 formation vs [O_2].


Figure 6. Absorption transient at 250 nm following the pulse radiolysis of a mixture of 40 mbar of CF_3CH_2Cl, 20 mbar of O_2, and 940 mbar of SF_6.
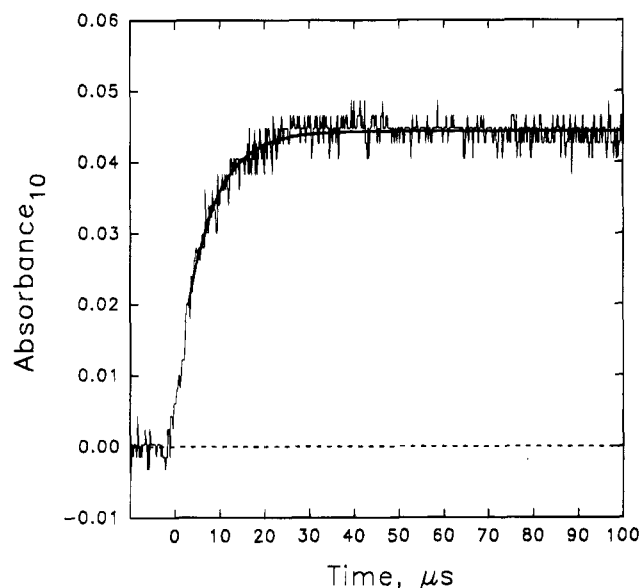
$(-k^1_s{}^1t)] + A_0$, where $A(t)$ is the absorbance as a function of time, A_∞ is the absorbance at infinite time, k^{1st} is the pseudo-first-order appearance rate of NO_2, and A_0 is the extrapolated absorbance at $t = 0$. The fit was started 3 μs after the radiolysis pulse to allow for the formation of the peroxy radical. A plot of the measured pseudo-first-order rate constant vs the NO concentration is shown in Figure 9. As seen from Figure 9, the pseudo-first-order rate constant, k^{1st}, increased linearly with [NO]. Linear least-squares analysis of the data in Figure 9 gives $k_3 = (1.0 \pm 0.3) \times 10^{-11}$ cm^3 molecule^{-1} s^{-1}, with an insignificant intercept of $(-0.26 \pm 3.95) \times 10^4$ s^{-1}.

The increase in absorbance at 400 nm can be combined with the literature value of σ(NO_2)(400nm) = 6.0 × 10^{-19} cm^2 molecule^{-1} (average of values over wavelength range given in ref 6) to calculate the yield of NO_2 in this system. The yield of NO_2 in the experiments given in Figure 9, expressed as moles of NO_2 produced per mole of F atoms consumed, was 97 ± 9%.

The CF_3CClHO_2 + NO_2 Reaction. Following the radiolysis of $CF_3CClH_2/NO_2/O_2/SF_6$ mixtures a decrease in the absorption was observed at 400 nm. This is ascribed to the loss of NO_2
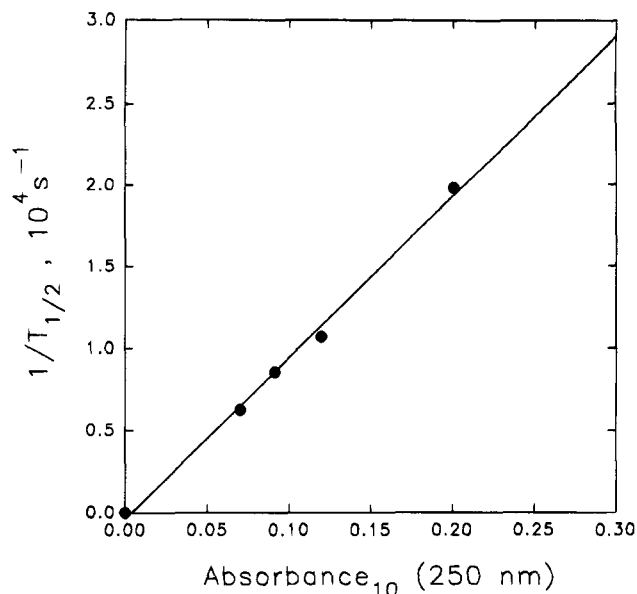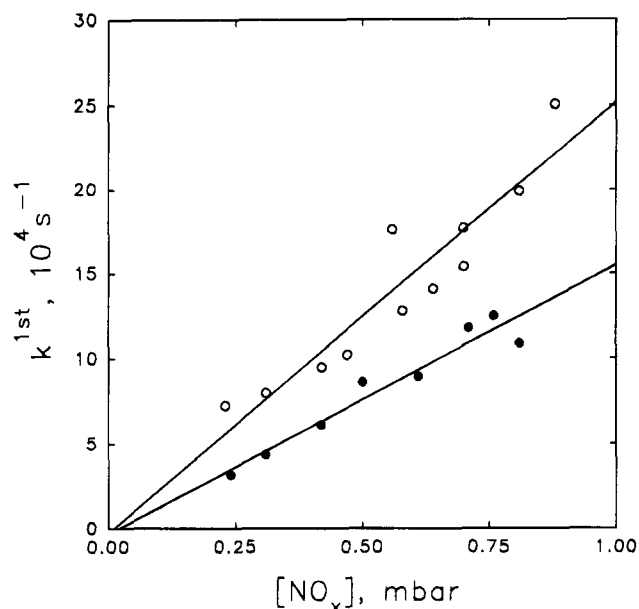
Figure 7. Reciprocal half-lives vs maximum absorbance at 250 nm for mixtures of 40 mbar of CF_3CH_2Cl, 20 mbar of O_2, and 940 mbar of SF_6.

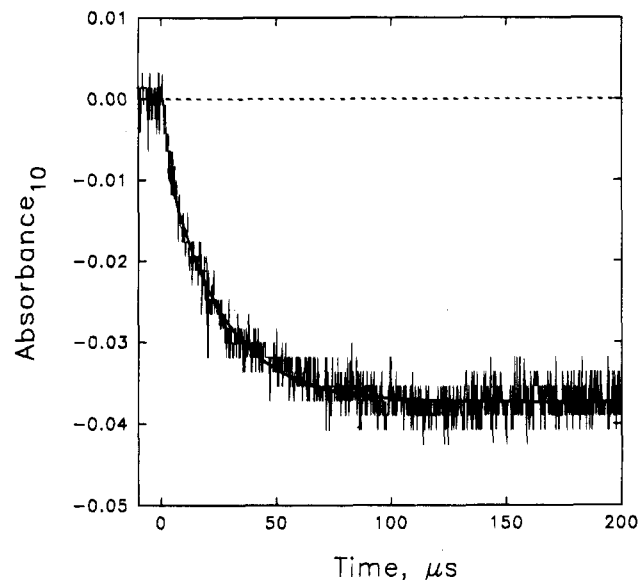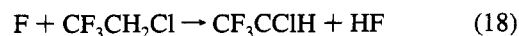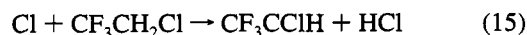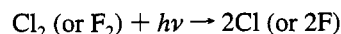**Figure 9.** Plot of k^{1st} [NO] (open symbols) and vs [NO$_2$] (closed symbols).

Figure 8. Transient absorbance at 400 nm observed following pulse radiolysis (dose = 50% of maximum) of a mixture of 0.64 mbar of NO, 40 mbar of CF_3CClH_2, 20 mbar of O_2, and 940 mbar of SF_6. The solid line is a first-order fit to the experimental data.
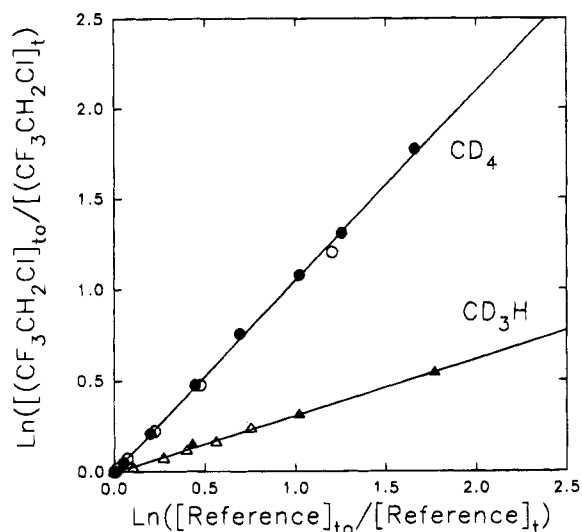

Figure 10. Transient absorbance at 400 nm observed following pulse radiolysis (dose = 50% of maximum) of a mixture of 0.31 mbar of NO$_2$, 40 mbar of CF_3CClH_2, 20 mbar of O_2, and 940 mbar of SF_6. The solid line is a first-order fit to the experimental data.

via reaction 4. An example of a typical experimental transient absorption is shown in Figure 10. The smooth solid line in Figure 10 is a first-order fit using the expression Abs(t) = (A_{inf} − C) × [1 − exp(−$k^{1st}t$)] + C, where Abs(t) is the absorbance as a function of time, A_{inf} is the absorbance at infinite time, k^{1st} is the pseudo-first-order loss rate of NO$_2$, and C is the extrapolated absorbance at $t = 0$. The decay was observed to follow first-order-kinetics in all cases. Of all the species initially present in the reaction cell only NO$_2$ absorbs significantly at 400 nm. Control experiments were performed in which SF_6/ CF_3CH_2Cl, SF_6/CF_3CH_2Cl/O_2, SF_6/O_2, or just SF_6 were radiolyzed; no change in absorption at 400 nm was observed. A plot of the measured pseudo-first-order decay rate vs the NO$_2$ concentration is shown in Figure 9. Linear least-squares analysis of the data in Figure 9 gives k_4 = (6.4 ± 1.5) × 10^{-12} cm^3 molecule^{-1} s^{-1}, with an insignificant intercept of (0.32 ± 1.96) × 10^{-4} s^{-1}. The decrease in absorption at 400 nm can be combined with value of σ_{NO_2} (400 nm) = 6.0 × 10^{-19} cm^2 molecule^{-1} [6] to calculate the loss of NO$_2$ in this system. The

loss of NO$_2$ in the experiments given in Figure 10, expressed as moles of NO$_2$ consumed per mole of F atoms consumed, was 93 ± 12%.

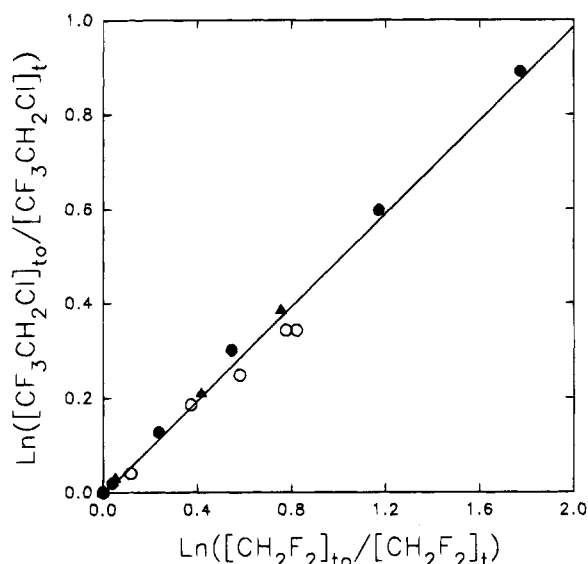**3.2. Results from FTIR−Smog Chamber System.** *Relative Rate Studies of the Reactions of Cl and F Atoms with CF$_3$-CH$_2$Cl.* Prior to investigating the atmospheric fate of CF$_3$-CClHO radicals, a series of relative rate experiments was performed using the FTIR system to investigate the kinetics of the reactions 15 and 8. The techniques used are described in detail elsewhere.[7] Photolysis of molecular halogen was used as a source of halogen atoms.

$$Cl_2 \text{ (or } F_2) + h\nu \rightarrow 2Cl \text{ (or } 2F)$$

$$Cl + CF_3CH_2Cl \rightarrow CF_3CClH + HCl \qquad (15)$$

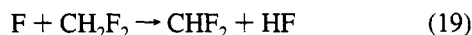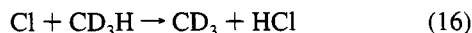$$F + CF_3CH_2Cl \rightarrow CF_3CClH + HF \qquad (18)$$

The kinetics of reaction 15 were measured relative to (16) and

Figure 11. Plot of the decay of CF_3CH_2Cl vs those of CD_4 and CHD_3 in 700 Torr of air (filled symbols) of nitrogen (open symbols) at 296 K in the presence of Cl atoms.

Figure 12. Plot of the decay of CF_3CH_2Cl vs that of CH_2F in 700 Torr of air (filled symbols) or nitrogen (open symbols) at 296 K in the presence of F atoms.
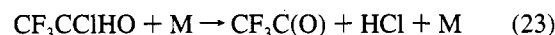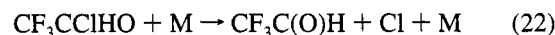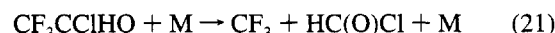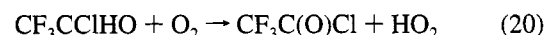
(17), reaction 8 was measured relative to (19).

$$Cl + CD_3H \rightarrow CD_3 + HCl \quad (16)$$

$$Cl + CD_4 \rightarrow CD_3 + DCl \quad (17)$$

$$F + CH_2F_2 \rightarrow CHF_2 + HF \quad (19)$$

The observed losses of CF_3CH_2Cl vs CD_3H and CD_4 in the presence of Cl atoms, and CF_3CH_2Cl vs CH_2F_2 in the presence of F atoms, are shown in Figures 11 and 12, respectively. There was no discernible difference between data obtained in 700 Torr of N_2 or air. In the study of the reaction of F atoms with CF_3-CH_2Cl care must be taken to avoid, or correct for, complications caused by the possible generation of Cl atoms following reaction 8. As a check for such complications, the initial concentration ratio $[CF_3CH_2Cl]/[CH_2F_2]$ was varied over the range 0.8–3.6 with no observable effect on the measured value of k_8/k_{19}. It seems reasonable to conclude that our measurement of k_8/k_{19} is free from any complications involving the formation of Cl atoms. Linear least-squares analyses of the data in Figures 11 and 12 give $k_{15}/k_{16} = 0.31 \pm 0.02$, $k_{15}/k_{17} = 1.05 \pm 0.05$, and $k_8/k_{19} = 0.49 \pm 0.04$. Using $k_{16} = 2.3 \times 10^{-14}$,[7] $k_{17} = 6.1 \times$

10^{-15},[7] and $k_{19} = 4.3 \times 10^{-12}$ [8] gives $k_{15} = (7.1 \pm 0.5) \times 10^{-15}$, $k_{15} = (6.4 \pm 0.3) \times 10^{-15}$, and $k_8 = (2.1 \pm 0.2) \times 10^{-12}$ cm^3 molecule^{-1} s$^{-1}$, respectively. We estimate that potential systematic errors associated with uncertainties in the reference rate constants could add additional 10 and 20% to the uncertainty ranges for k_{15} and k_8, respectively. Propagating this additional uncertainty gives values of $k_{15} = (7.1 \pm 0.9) \times 10^{-15}$, $k_{15} = (6.4 \pm 0.7) \times 10^{-15}$, and k_8 $(2.1 \pm 0.5) \times 10^{-12}$ cm^3 molecule^{-1} s^{-1}. We choose to cite a final value of k_{15} which is an average of those determined using the two different reference compounds together with error limits which encompass the extremes of the two individual determinations. Hence, $k_{15} = (6.8 \pm 1.2) \times 10^{-15}$ cm^3 molecule^{-1} s^{-1}. The quoted error reflects the accuracy of the measurements. The value of k_8 determined using the FTIR technique is in good agreement with the determination of $k_8 = (2.0 \pm 0.6) \times 10^{-12}$ cm^3 molecule^{-1} s^{-1} using the pulse radiolysis technique in the present work. There are no literature data for k_8 with which to compare our results. The value of k_{15} reported herein is consistent with the experimental uncertainties with the previous absolute measurement of $k_{15} = 5.9 \times 10^{-15}$ cm^3 molecule^{-1} s^{-1} by Jourdain et al.[9] The consistency in the values of k_8 measured using the pulse radiolysis and FTIR relative rate techniques suggests the absence of any significant reactive impurities in the sample of CF_3CH_2Cl used in this work.

Study of the Atmospheric Fate of CF_3CClHO Radicals. To determine the atmospheric fate of the alkoxy radical CF_3CClHO experiments were performed in which $CF_3CH_2Cl/O_2/Cl_2$ and $CF_3CH_2Cl/O_2/F_2$ mixtures at a total pressure of 700 Torr made up with N_2 diluent were irradiated in the FTIR–smog chamber system. The loss of CF_3CH_2Cl and the formation of products were monitored by FTIR spectroscopy. CF_3CClHO radicals formed in the chamber in reaction 6a will either react with O_2 to give the aldehyde $CF_3C(O)Cl$ (reaction 20), dissociate to give $HC(O)Cl$ and CF_3 radicals (reaction 21), eliminate a Cl atom to give CF_3CHO (reaction 22), or undergo intramolecular HCl elimination to give CF_3CO radicals (reaction 23).

$$CF_3CClHO_2 + CF_3CClHO_2 \rightarrow 2CF_3CClHO + O_2 \quad (6a)$$

$$CF_3CClHO_2 + CF_3CClHO_2 \rightarrow$$
$$CF_3CClHOH + CF_3C(O)Cl + O_2 \quad (6b)$$

$$CF_3CClHO + O_2 \rightarrow CF_3C(O)Cl + HO_2 \quad (20)$$

$$CF_3CClHO + M \rightarrow CF_3 + HC(O)Cl + M \quad (21)$$

$$CF_3CClHO + M \rightarrow CF_3C(O)H + Cl + M \quad (22)$$

$$CF_3CClHO + M \rightarrow CF_3C(O) + HCl + M \quad (23)$$
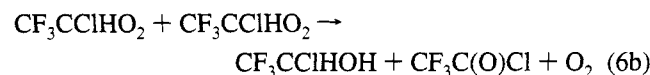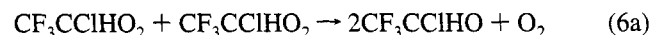
CF_3 radicals formed in reaction 21 are expected to be converted into CF_3OH via addition of O_2, reaction with peroxy radicals (CF_3CClHO_2 or CF_3O_2) to give CF_3O radicals, which will then abstract a H atom from CF_3CH_2Cl.

The observed products formed during the oxidation of CF_3-CH_2Cl were $CF_3C(O)Cl$, CO, CO_2, CF_3OH, and HCl. Let us consider $CF_3C(O)Cl$. Figure 13 shows the results obtained from the UV irradiation of three different $CF_3CH_2Cl/Cl_2/N_2/O_2$ mixtures. As seen in Figure 13, the observed formation of $CF_3C(O)Cl$ was a linear function of the CF_3CH_2Cl loss. Such linearity suggests, but does not prove, that secondary loss of $CF_3C(O)Cl$ is not a complication in this work. To provide information on the behavior of $CF_3C(O)Cl$ in the chamber, mixtures of $CF_3C(O)Cl$ in air, with and without added Cl_2, were prepared, allowed to stand in the dark for 5 min and then

Atmospheric Chemistry of HCFC-133a

J. Phys. Chem., Vol. 99, No. 36, 1995 **13443**
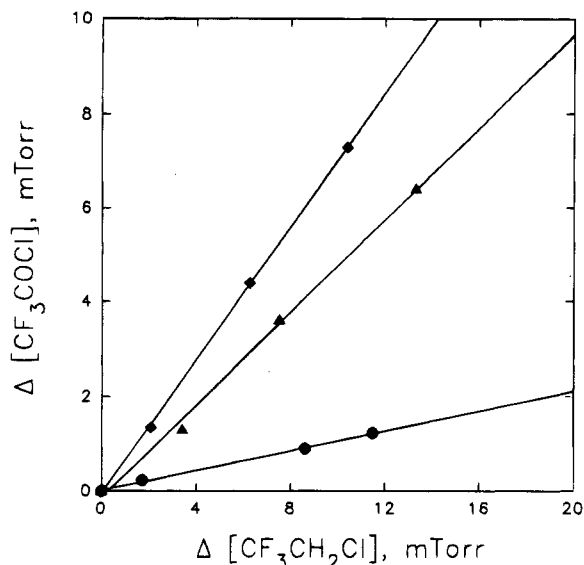
Figure 13. Formation of $CF_3C(O)Cl$ as a function of the loss of CF_3-CH_2Cl following the irradiation of mixtures of 98—100 mTorr of CF_3-CH_2Cl, 0.4—0.5 Torr of Cl_2, and 2.38 Torr (circles), 147 Torr (triangles), or 700 Torr of O_2 (diamonds) in 700 Torr total pressure made up where appropriate with N_2 diluent.
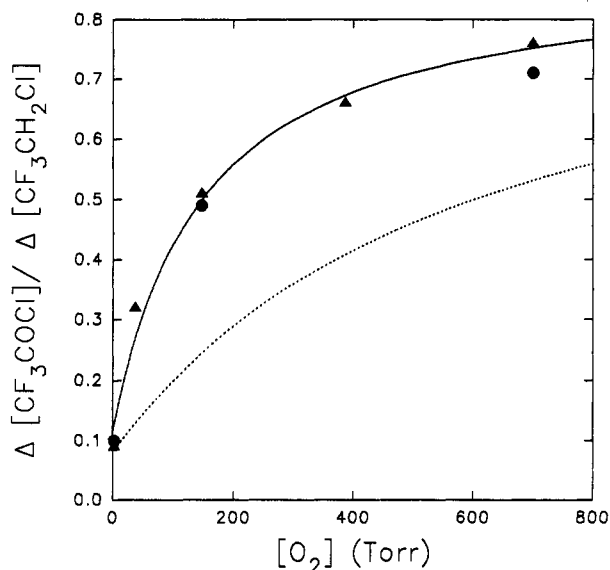
Figure 14. Observed yield of $CF_3C(O)Cl$ following F atom (triangles) or Cl atom (circles) initiated oxidation of CF_3CH_2Cl in 700 Torr total pressure of N_2/O_2 as a function of the O_2 partial pressure. The solid line is a fit to the data, see text for details. The dotted line represents the observed yield of $CF_3C(O)F$ following Cl atom initiated oxidation of CF_3CH_2F taken from ref 12.

irradiated for 5 min. No loss (<1%) of $CF_3C(O)Cl$ was discernible suggesting that under the present experimental conditions, $CF_3C(O)Cl$ is not lost by heterogeneous processes, photolysis, or reaction with Cl atoms. Linear least-squares analysis of the data in Figure 13 provides molar yields of CF_3C-$(O)Cl$. A series of experiments was performed using a range of O_2 partial pressures all at 700 Torr total pressure with N_2 diluent. Both Cl and F atom initiation were employed. As seen from Figure 14, the molar yield of $CF_3C(O)Cl$ was found to increase with increasing O_2 partial pressure. Experiments employing Cl and F atom initiation gave indistinguishable results. There are two known sources of $CF_3C(O)Cl$ in the present experiments: reactions 6b and 20. The fact that the $CF_3C(O)Cl$ yield is O_2 dependent shows that loss mechanisms other than reaction 20 compete for the available CF_3CClHO radicals. A reasonable question at this point is "What other loss mechanism(s) competes for CF_3CClHO radicals?" As

discussed above, three possibilities exist: reactions 21, 22, or 23. Unfortunately, on the basis of the present experiments we are unable to determine the relative importance of these reactions. The problem lies in unavoidable secondary reactions of $HC(O)Cl$ and $CF_3C(O)H$ which serve as markers for reactions 21 and 22, respectively. IR features attributable to $HC(O)Cl$ (<0.2 mTorr) and $CF_3C(O)H$ (<1.5 mTorr) were searched for but not found. However, the absence of significant quantities of these carbonyl products does not prove that reactions 21 and 22 are unimportant. $HC(O)Cl$ and CF_3CHO (if formed) are likely to be consumed by secondary reactions involving Cl atoms (in all experiments), F atoms (in those experiments employing F atom initiation), or CF_3O radicals (in all experiments). Kinetic data are available concerning the reactivity of CF_3CHO towards F and Cl atoms,[10] $HC(O)Cl$ toward Cl atoms,[11] and CF_3CH_2Cl toward F and Cl atoms (this work). Hence, estimates of the importance of such secondary reactions can be provided. Compared to CF_3CH_2Cl, CF_3CHO is more reactive toward F and Cl atom attack by factors of 265 and 13, respectively, and $HC(O)Cl$ is more reactive toward Cl atoms by a factor of 115. The reactivity of F atoms toward $HC(O)Cl$ is unknown but might reasonably be expected to be substantially greater than that toward CF_3CH_2Cl. Similarly, the reactivity of CF_3O radicals toward CF_3CHO and $HC(O)Cl$ has not been reported but is likely to be greater than that toward CF_3CH_2Cl. Potential complications associated with secondary chemistry can be reduced by increasing the initial concentrations and using low conversions (<1%) of CF_3CH_2Cl. This course of action was not pursued because the stated purity of the CF_3CH_2Cl used was >99%, hence if conversions of <1% were employed it would be impossible to guarantee that the observed products were not merely attributable to chemistry involving impurities in the CF_3CH_2Cl sample. Secondary chemistry is unavoidable in the present experiments and precludes the identification of loss mechanisms for CF_3CClHO radicals other than reaction 20.

The dependence of $CF_3C(O)Cl$ yield on O_2 partial pressure shown in Figure 14 is reminiscent of that of $CF_3C(O)F$ from CF_3CFHO radicals.[12] The dotted line in Figure 14 is the $CF_3C(O)F$ yield observed following irradiation of $CF_3CH_2F/$ $Cl_2/N_2/O_2$ mixtures at 700 Torr total pressure.[12] As discussed previously,[12] the simplest chemical mechanism that explains the observed dependence of the $CF_3C(O)Cl$ product yield on the O_2 partial pressure consists of (6a), (6b), (20), and (21) (we ignore for the moment reactions 22 and 23). Using this chemical mechanism, it can be shown that the dependence of the molar yield of $CF_3C(O)Cl$ should follow the expression

$$CF_3C(O)Cl \text{ yield} = Y_0 + (1 - 2Y_0)(\{(k_{20}/k_{21})[O_2]\}/\{1 + (k_{20}/k_{21})[O_2]\}) \quad (I)$$

where Y_0 is the $CF_3C(O)Cl$ yield extrapolated to zero oxygen pressure, k_{20} is the bimolecular rate constant for reaction 20, k_{21} is the unimolecular rate constant for reaction 21, and [O_2] is the partial pressure of oxygen. The solid line in Figure 14 is a fit of expression I to the observed $CF_3C(O)Cl$ yield. As seen from Figure 14, the dependence of the $CF_3C(O)Cl$ yields on [O_2] is well described by expression I. The least-squares fit to the data in Figure 14 gives $Y_0 = 0.11 \pm 0.04$, and $k_{20}/k_{21} = (2.1 \pm 0.4) \times 10^{-19}$ cm^3 molecule^{-1}. The analogous data for CF_3CFHO radicals (given by the dotted line in Figure 14) gave Y_0 (for CF_3CFHO_2 radicals) = 0.08 ± 0.03 and $k(CF_3CFHO + O_2 \rightarrow CF_3C(O)F + HO_2)/k(CF_3CFHO \rightarrow CF_3 + HC(O)F) = (5.1 \pm 0.7) \times 10^{-20}$ cm^3 molecule^{-1}. The values of Y_0, which provide measures of the importance of the molecular channel (i.e., (6b)) in the self-reactions of CF_3CClHO_2 and CF_3CFHO_2 radicals, are indistinguishable. For a given O_2 partial pressure,

CF_3CClHO radicals are approximately 4 times more prone to reaction with O_2 than are CF_3CFHO radicals.

The atmospheric chemistry of CF_3CFHO radicals has been studied extensively and it has been established that reaction with O_2 (giving $CF_3C(O)F$ and HO_2 radicals) competes with C–C bond scission (giving CF_3 radicals and $HC(O)F$.[12–14] In light of the similar dependencies of $CF_3C(O)X$ (X = Cl or F) yields on the O_2 partial pressure, we believe (but can not prove) that C–C bond scission (i.e., reaction 21) is the loss process that competes for CF_3CClHO radicals in the present experiments. In the rest of this paper we proceed on the assumption that reactions 22 and 23 are of negligible importance.

The data in Figure 14 shows that the competition between reaction with O_2 and decomposition is tilted more toward reaction with O_2 for CF_3CClHO radicals than for CF_3CFHO radicals. This observation implies either a strengthening of the C–C bond in CF_3CClHO radicals compared to CF_3CFHO, or a weakening of the C–H bond, or both. Barry et al.[15] have noted that in the series of alkoxy radicals of the general formula CX_3CFHO (where X = H or F) the importance of reaction with O_2 compared to C–C bond scission increases with the polarity of the C–C bond. This behavior was ascribed to an increase in C–C bond strength with increasing polarity. Since CF_3-$CClHO$ radicals are more polar than CF_3CFHO radicals the increased importance of reaction with O_2 in the atmospheric chemistry of CF_3CClHO radicals supports the hypothesis by Barry et al.[15] Finally, before we leave this section it is relevant note that as seen in Figure 14 the same product yields were observed using either F or Cl atom initiation. This suggests that CF_3CHCl radicals are formed as the major, if not sole, product of reaction of F atoms with CF_3CH_2Cl.

4. Discussion

Following release into the atmosphere, CF_3CH_2Cl will react predominantly with hydroxyl radicals. The atmospheric lifetime of CF_3CH_2Cl with respect to reaction with OH is 4–5 years.[16] Reaction with OH gives CF_3CClH radicals which are rapidly (within 1 μs), converted into the corresponding peroxy radical, CF_3CClHO_2. Using $k_3 = 1.0 \times 10^{-11}$ cm^3 molecule^{-1} s^{-1} together with an estimated background tropospheric NO concentration of 2.5×10^8 cm^{-3},[17] the lifetime of CF_3CClHO_2 radicals with respect to reaction 3 is calculated to be 7 min. Reaction 3 is likely to be an important atmospheric loss of CF_3-$CClHO_2$ radicals. We have shown here that CF_3CClHO_2 radicals react with NO to produce NO_2 and (by inference) CF_3-$CClHO$ radicals.

Decomposition and reaction with O_2 are both important loss mechanisms for CF_3CClHO radicals at 296 K and 700 Torr total pressure of N_2 diluent. Decomposition probably gives CF_3 radicals and $HC(O)Cl$. At 296 K, the rate constant ratio $k_{20}/k_{21} = (2.1 \pm 0.4) \times 10^{-19}$ cm^3 molecule^{-1}. In 1 atm of air at 296 K, decomposition and reaction with O_2 are of approximately equal importance. In the earth's atmosphere the temperature is generally substantially lower than 296 K. The rates of reactions 20 and 21 will both decrease with decreasing temperature. Reaction 21 is a unimolecular decomposition and will be particularly sensitive to temperature. The average temperature of air between 0 and 10 km is 278 K.[18] If we assume that the difference in activation energies for reactions 20 and 21 is the same as that for the analogous reactions of CF_3CFHO radicals (i.e., 7.2 kcal mol^{-1} [12]), then the rate constant ratio k_{20}/k_{21} will be a factor of 2 lower at 278 K than at 296 K. We must consider the impact of decreasing total pressure and oxygen partial pressure with increasing altitude. The rate constant ratio $k_{20}/k_{21} = (2.1 \pm 0.4) \times 10^{-19}$ cm^3 molecule^{-1} reported here is appropriate for 700 Torr total pressure. k_{21} is expected to be

sensitive to the total pressure while k_{20} is not, and the ratio k_{20}/k_{21} will increase as pressure is decreased. By analogy to the observed behavior of CF_3CFHO radicals,[12] the effects of decreasing total pressure and decreasing O_2 concentration with increasing altitude will approximately cancel out. We conclude that reaction with O_2 is the dominant fate of CF_3CClHO radicals, with decomposition via C–C bond scission making a minor, but nonnegligible, contribution. In the troposphere, $CF_3C(O)Cl$ will be incorporated into rain–cloud–sea water and undergo hydrolysis to CF_3COOH which will then be rained out.[19] The atmospheric degradation products of HCFC-133a have lifetimes substantially less than that of the parent compound and are incapable of transporting significant amounts of chlorine to the stratosphere. $CF_3C(O)Cl$ produced in the upper stratosphere will photolyze to give CF_3 + CO + Cl.[20–22]

References and Notes

(1) Sehested, J.; Nielsen, O. J.; Wallington, T. J. *Chem. Phys. Lett.* **1993**, *213*, 457.

(2) Ellermann, T. Risø-M-2932, 1991.

(3) Wallington, T. J.; Japar, S. M. *J. Atmos. Chem.* **1989**, *9*, 399.

(4) Sehested, J.; Sehested, K.; Nielsen, O. J.; Wallington, T. J. *J. Phys. Chem.* **1994**, *98*, 6731.

(5) Ellermann, T.; Sehested, J.; Nielsen, O. J.; Pagsberg, P.; Wallington, T. J. *Chem. Phys. Lett.* **1993**, *218*, 287.

(6) DeMore, W. B.; Sander, S. P.; Golden, D. M.; Hampson, R. F.; Kurylo, M. J.; Howard, C. J.; Ravishankara, A. R.; Kolb, C. E.; Molina, M. J. Jet Propulsion Laboratory Publication 92-20, Pasadena, CA, 1992.

(7) Wallington, T. J.; Hurley, M. D. *Chem. Phys. Lett.* **1992**, *189*, 437.

(8) Wallington, T. J.; Hurley, M. D.; Shi, J.; Maricq, M. M.; Sehested, J.; Nielsen, O. J.; Ellermann, T. *Int. Chem. Kinet.* **1993**, *25*, 651.

(9) Jourdain, J.-L.; Le Bras, G.; Combourieu, J. *J. Chim. Phys.* **1978**, *75*, 318.

(10) Wallington, T. J.; Hurley, M. D. *Int. J. Chem. Kinet.* **1993**, *25*, 819.

(11) Niki, H.; Maker, P. D.; Savage, C. M.; Breitenbach, L. P. *Int. J. Chem. Kinet.* **1980**, *12*, 915.

(12) Wallington, T. J.; Hurley, M. D.; Ball, J. C.; Kaiser, E. W. *Environ. Sci. Technol.* **1992** *26*, 1318.

(13) Tuazon, E. C.; Atkinson, R. *J. Atmos. Chem.* **1993**, *16*, 301.

(14) Rattigan, O. V.; Rowley, D. M.; Wild, O.; Jones, R. L.; Cox, R. A. *J. Chem. Soc., Faraday Trans.* **1994**, *90*, 1819.

(15) Barry, J.; Sidebottom, H. W.; Treacy, J. *Abstract Book for 13th International Symposium on Gas Kinetics*; University College: Dublin, Ireland, 1994; p 327.

(16) Derwent, R. G.; Volz-Thomas, A.; Prather, M. J. World Meteorological Organization Global Ozone Research and Monitoring Project, Report No. 20; Scientific Assessment of Stratospheric Ozone, 1989; Vol. 2, p 124.

(17) Atkinson, R., World Meteorological Organization Global Ozone Research and Monitoring Project, Report No. 20; Scientific Assessment of Stratospheric Ozone, 1989, Vol. 2, p 167.

(18) Brasseur, G.; Solomon, S. *Aeronomy of the Middle Atmosphere*; Reidel: Dordrecht, The Netherlands, 1986.

(19) Wallington, T. J.; Schneider, W. F.; Worsnop, D. R.; Nielsen, O. J.; Sehested, J.; DeBruyn, W. J.; Shorter, J. A. *Environ. Sci. Technol.* **1994**, *28*, 320A.

(20) Rattigan, O. V.; Wild, O.; Jones, R. L.; Cox, R. A. *J. Photochem. Photobiol. A: Chem.* **1993**, *71*, 1.

(21) Meller, R.; Boglu, D.; Moortgat, G. K. *Proceedings of the STEP-HALOCSIDE/AFEAS Workshop*; University College: Dublin, Ireland, March 1993; p 130.

(22) Maricq, M. M.; Szente, J. J. *J. Phys. Chem.*, submitted for publication.